⌘ *Author's Choice*

THE JOURNAL OF BIOLOGICAL CHEMISTRY VOL. 283, NO. 46, pp. 31763–31775, November 14, 2008

Synaptotagmin C2B Domain Regulates Ca^{2+}-triggered Fusion *in Vitro*

CRITICAL RESIDUES REVEALED BY SCANNING ALANINE MUTAGENESIS[*S]

Received for publication, May 1, 2008, and in revised form, September 3, 2008 Published, JBC Papers in Press, September 10, 2008, DOI 10.1074/jbc.M803355200

Jon D. Gaffaney, F. Mark Dunning, Zhao Wang, Enfu Hui, and Edwin R. Chapman[1]

From the Department of Physiology and Howard Hughes Medical Institute, University of Wisconsin, Madison, Wisconsin 53706

Synaptotagmin (syt) 1 is localized to synaptic vesicles, binds Ca^{2+}, and regulates neuronal exocytosis. Syt 1 harbors two Ca^{2+}-binding motifs referred to as C2A and C2B. In this study we examine the function of the isolated C2 domains of Syt 1 using a reconstituted, SNARE (soluble *N*-ethylmaleimide-sensitive factor attachment receptor)-mediated, fusion assay. We report that inclusion of phosphatidylethanolamine into reconstituted SNARE vesicles enabled isolated C2B, but not C2A, to regulate Ca^{2+}-triggered fusion. The isolated C2B domain had a 6-fold lower EC_{50} for Ca^{2+}-activated fusion than the intact cytosolic domain of Syt 1 (C2AB). Phosphatidylethanolamine increased both the rate and efficiency of C2AB- and C2B-regulated fusion without affecting their abilities to bind membrane-embedded syntaxin-SNAP-25 (t-SNARE) complexes. At equimolar concentrations, the isolated C2A domain was an effective inhibitor of C2B-, but not C2AB-regulated fusion; hence, C2A has markedly different effects in the fusion assay depending on whether it is tethered to C2B. Finally, scanning alanine mutagenesis of C2AB revealed four distinct groups of mutations within the C2B domain that play roles in the regulation of SNARE-mediated fusion. Surprisingly, substitution of Arg-398 with alanine, which lies on the opposite end of C2B from the Ca^{2+}/membrane-binding loops, decreases C2AB t-SNARE binding and Ca^{2+}-triggered fusion *in vitro* without affecting Ca^{2+}-triggered interactions with phosphatidylserine or vesicle aggregation. In addition, some mutations uncouple the clamping and stimulatory functions of syt 1, suggesting that these two activities are mediated by distinct structural determinants in C2B.

In nerve terminals, synaptic vesicles (SVs)[2] are loaded with neurotransmitter, docked at active zones, and primed for exocytosis. Increases in intracellular [Ca^{2+}] then trigger the synchronous fusion of docked SVs with the plasma membrane, releasing transmitters into the synaptic cleft (1). The fusion step is thought to be mediated by SNARE proteins that form the core of a conserved membrane fusion machine. The SV SNARE complex consists of the vesicle protein (v-SNARE) synaptobrevin (syb), and the target membrane proteins (t-SNAREs) syntaxin 1 and SNAP-25 (2). A current challenge is to understand how the SNARE complex is regulated such that it drives fusion, in response to Ca^{2+} influx, on the microsecond to millisecond time scale.

Syt 1 is localized to synaptic vesicles and large dense-core granules in neurons and neuroendocrine cells and is thought to function as a Ca^{2+} sensor for rapid synchronous release of neurotransmitter (3). Structurally, syt 1 consists of a short luminal tail, a single transmembrane domain, and a cytosolic region comprising two C2 domains, C2A and C2B, connected by a short linker (4). In response to binding Ca^{2+}, both C2 domains of syt 1 partially penetrate into lipid bilayers that contain anionic phospholipids such as phosphatidylserine (PS) (5–7); these interactions play a critical role during membrane fusion (8). In addition, syt 1 binds to the t-SNAREs, syntaxin and SNAP-25, in a Ca^{2+}-regulated manner (9–11), and these interactions are also thought to play a role in excitation-secretion coupling (3, 8, 11, 12), although this point is not universally accepted (13–15). An early model, bolstered by more recent data, indicates that syt 1 might act as a switch by clamping fusion under resting conditions and then accelerating fusion in response to Ca^{2+} (3, 16, 17).

Reconstitution experiments, using vesicles that harbor syb and vesicles that harbor syntaxin-SNAP-25 heterodimers, demonstrated that SNAREs are sufficient to mediate membrane fusion *in vitro*. However, fusion was slow and relatively inefficient (18). Addition of the cytosolic domain of syt 1 (C2AB), to the *in vitro* SNARE-mediated fusion assay, conferred Ca^{2+} sensitivity to the reaction and increased the rate and efficiency of fusion (17, 19). It was further demonstrated that C2AB was able to drive assembly of SNAP-25 onto membrane-embedded syntaxin, resulting in SNARE complexes that are competent to drive membrane fusion (20). These data demonstrate that Ca^{2+}·C2AB is able to influence the structure and

* This work was supported, in whole or in part, by National Institutes of Health Grants GM 56827 and MH 61876. This work was also supported by American Heart Association Grant 0440168N. The costs of publication of this article were defrayed in part by the payment of page charges. This article must therefore be hereby marked "*advertisement*" in accordance with 18 U.S.C. Section 1734 solely to indicate this fact.

⌘ *Author's Choice*—Final version full access.

[S] The on-line version of this article (available at http://www.jbc.org) contains supplemental Figs. S1–S5.

[1] An Investigator of the Howard Hughes Medical Institute. To whom correspondence should be addressed: 1300 University Ave., 129 SMI, Madison, WI 53706. Tel.: 608-263-5512; Fax: 608-265-5512; E-mail: chapman@physiology.wisc.edu.

[2] The abbreviations used are: SV, synaptic vesicle; SNARE, soluble *N*-ethylmaleimide-sensitive factor attachment protein receptor; syt 1, full-length synaptotagmin 1; C2AB, cytosolic domain of syt 1; C2A, membrane proximal C2 domain of syt 1; C2B, membrane distal C2 domain of syt 1; NBD-PE, 1,2-dipalmitoyl-*sn*-glycero-3-phosphoethanolamine-*N*-(7-nitro-2–1,3-benzoxadiazol-4-yl); Rhodamine-PE, 1,2-dipalmitoyl-*sn*-glycero-3-phosphoethanolamine-*N*-(lissamine rhodamine B sulfonyl); PS, 1,2-dioleoyl-*sn*-glycero-3-[phospho-L-serine]; PC, 1-palmitoyl-2-oleoyl-*sn*-glycero-3-phosphocholine; PE, 1-palmitoyl-2-oleoyl-*sn*-glycero-3-phosphoethanolamine; wt, wild type; syb, synaptobrevin.

function of SNAREs and that C2AB is able to directly couple Ca^{2+} influx to vesicle fusion.

There are apparent disparities between data obtained from cell-based model systems as opposed to reconstituted fusion assays, relating to the relative importance that each C2 domain of syt 1 plays during fusion. Several studies concluded that the C2B domain, but not the C2A domain, is critical for syt 1 function in neurons. For example, mutations that completely abolish the Ca^{2+}-sensing ability of C2A appear to have little effect on synaptic transmission, whereas similar mutations in C2B completely disrupt function (21–24). Moreover, deletion of the C2B domain dramatically reduced secretion in *Drosophila* mutants, and a point mutation in this domain shifted the Ca^{2+} dose response to the right (25). Finally, substitution of basic resides within C2B results in diminished t-SNARE binding activity and synaptic transmission (11, 26, 27). Although cell-based experiments indicate that C2B is the major determinant that enables syt to regulate fusion, in all published studies, the isolated C2B domain had no effect in the reconstituted fusion assay (19, 28, 29).

A second question concerns the interaction of syt 1 with SNARE proteins. Initial studies, as well as recent biophysical measurements, mapped this interaction largely to the C2B domain of syt 1 (30, 31). However, this is not a completely resolved issue, as others have suggested that isolated C2A mediates the t-SNARE-binding activity of syt 1 (32, 33). Indeed, a recent study used zero-length cross-linking between SNAP-25 and C2AB to identify residues within C2A that mediated Ca^{2+}-dependent binding (12). In addition, neutralization of the positively charged residues R233Q and K366Q in the Ca^{2+}-binding membrane penetration loops of C2A and C2B, respectively, reduce binding of C2AB to membranes and SNAP-25, indicating that these residues may make contacts between both the SNAREs and membranes during vesicle fusion (34). The emerging view is that both C2 domains participate in interactions with t-SNAREs, but C2B plays a more significant role in binding (3).

Other than the handful of domain mapping studies summarized above, relatively little is known regarding the precise interfaces that mediate the interaction of syt with t-SNAREs. High resolution structures for the C2 domains of syt 1, and for the core of the SNARE complex, have been determined, thus providing a framework to address this question via in-depth mutagenesis and modeling (35–37).

In this study, we demonstrate for the first time that the isolated C2B domain of syt 1 is able to drive Ca^{2+}-dependent membrane fusion in the reconstituted SNARE-mediated fusion assay; isolated C2A had little effect. C2B-regulated fusion was strictly dependent upon the presence of PE in the reconstituted vesicles; PE also dramatically increased the rate of fusion regulated by C2AB. To further refine the regions in C2AB that are important for regulated fusion, we carried out scanning alanine mutagenesis of residues within both the C2A and C2B domains. This analysis revealed several mutations within the C2B domain of syt 1 that reduced Ca^{2+}-dependent liposome fusion. In particular, Arg-398, which lies at the opposite end of C2B as the membrane penetration loops, appears to play an important role in syt-t-SNARE interactions and membrane fusion. Together, these results highlight the role of C2B in SNARE-catalyzed Ca^{2+}-dependent fusion and identify a new region of C2B that is critical for syt 1 function during fusion.

EXPERIMENTAL PROCEDURES

Plasmid Constructs—Plasmids for mouse synaptobrevin 2 and the t-SNARE heterodimer (mouse SNAP-25B and rat syntaxin 1A), were kindly provided by J. E. Rothman, Columbia University, New York. C2A, C2B, and C2AB were expressed in pGEX-2T or -4T as described previously (38). Syb and the t-SNARE complex were expressed as previously described (18, 19). The overlapping primer method was used to generate site-directed point mutations in a modified pTrcHisA construct containing the syt 1 C2AB domain (amino acids 95–421). This modified pTrcHisA vector has the gene 10-leader, Xpress Epitope, and enterokinase recognition and cleavage site removed.

Protein Expression and Purification—To generate His-tagged syb and t-SNARE heterodimers, *Escherichia coli* were grown at 37 °C to an A_{600} of 0.8, and protein expression was induced with 0.4 mM isopropyl 1-thio-β-D-galactopyranoside. Four hours after induction the bacteria were collected by centrifugation, and the pellet was resuspended in resuspension buffer (25 mM HEPES-KOH, 400 mM KCl, 20 mM imidazole, and 5 mM 2-mercaptoethanol). Resuspended bacteria were subjected to sonication (2 × 45 s, 50% duty cycle). Triton X-100 (2%), protease inhibitors (1 mg of aprotinin, pepstatin, and leupeptin; 0.5 mM phenylmethylsulfonyl fluoride), and 0.1 mg/ml RNase and DNase were added to the sonicated material, and the mixture was incubated for 2–3 h with rotation at 4 °C. Insoluble material was removed by centrifugation (Beckman JA17 rotor, 17K rpm), and the supernatant was applied to a Ni^{2+} column using an AktaFPLC™ (GE-Amersham Biosciences). The column was washed extensively with resuspension buffer containing 1% Triton X-100 and then 1% *n*-octylglucoside wash buffer (25 mM HEPES-KOH, 400 mM KCl, 50 mM imidazole, 10% glycerol, 5 mM 2-mercaptoethanol, 1% *n*-octylglucoside). The bound protein was eluted using *n*-octylglucoside wash buffer with 500 mM imidazole.

For the C2AB point mutants, *E. coli* were grown as above, however, following addition of isopropyl 1-thio-β-D-galactopyranoside bacteria were grown for an additional 4 h at 30 °C. Bacteria were collected by centrifugation, resuspended in His_6 buffer (25 mM HEPES-KOH, 500 mM NaCl, 20 mM imidazole), and sonicated as mentioned above. Samples were incubated with 1% Triton X-100 and protease inhibitors for 1 h followed by centrifugation to remove the insoluble material. The supernatant was incubated with Ni^{2+}-Sepharose HP beads overnight. The following day, the Ni^{2+} beads were washed with 20 volumes of His_6 buffer containing 1 M NaCl, 20 volumes His_6 buffer supplemented with 0.1 mg/ml RNase and DNase, and eluted with 1.5 volumes of elution buffer (25 mM HEPES-KOH, 500 mM NaCl, 500 mM imidazole). Eluted protein was dialyzed against 50 mM HEPES-KOH, 150 mM NaCl, and 10% glycerol.

For glutathione *S*-transferase-tagged proteins, *E. coli* were grown as described above for the point mutants. However, they were resuspended in phosphate buffered-saline containing 10% glycerol and 1 mM dithiothreitol. Bacteria were sonicated, treated with Triton X-100, and protease inhibitors. Insoluble

material was removed as described. The supernatant was collected, and incubated overnight at 4 °C with glutathione-Sepharose beads with rotation. Beads were washed extensively with phosphate buffered-saline (10% glycerol, 1 mM dithiothreitol) containing 0.1 mg/ml RNase and DNase, and the protein was removed by thrombin cleavage (50 units/ml of bead slurry for 2 h at 20 °C). The supernatant was collected and treated with phenylmethylsulfonyl fluoride to inactivate the thrombin.

All proteins were analyzed by SDS-PAGE and stained with Coomassie Blue to determine the purity and concentration against a bovine serum albumin standard curve. The concentration of C2A, C2B, and C2AB was verified using a BCA protein assay kit compatible with reducing agents.

Protein Reconstitution—Vesicles were prepared as described previously (19). Briefly, lipids supplied in chloroform were combined in various molar ratios (t-SNARE vesicles: 15% PS, 30% PE, 55% PC; v-SNARE vesicles: 15% PS, 27% PE, 55% PC, 1.5% NBD-PE, 1.5% Rhodamine-PE), dried under a stream of nitrogen, and subjected to vacuum for >1 h. Proteins to be reconstituted were diluted in elution buffer to yield ~100 copies per vesicle. Syb was diluted to 0.19 mg/ml and the syntaxin·SNAP-25 complex was diluted to 0.8 mg/ml in elution buffer. The dried lipid film was solubilized using these respective protein mixes and subsequently diluted with reconstitution buffer (25 mM HEPES-KOH, 100 mM KCl, 10% glycerol, 1 mM dithiothreitol). Protein-free vesicles were prepared as described above; however, the protein was omitted.

Vesicles were dialyzed against reconstitution buffer overnight, changing the buffer once. The dialyzed vesicles were collected, mixed with 80% Accudenz, and transferred into ultra clear centrifuge tubes. A step gradient was prepared by addition of 30 and 0% Accudenz layers onto the vesicle layer. The samples were centrifuged at 41,000 rpm for 5 h (SW-41 rotor) or 55,000 rpm for 1.75 h (SW-55 rotor). Vesicles were collected from the 0–30% interface and analyzed by SDS-PAGE to verify protein incorporation.

Fusion Assays and Data Analysis—Fusion assays were carried out in white-bottom 96-well plates with total reaction volumes of 75 μl. Each reaction contained 45 μl of t-SNARE vesicles or protein-free vesicles, 5 μl of NBD-Rhodamine-labeled v-SNARE vesicles, and 1.5 μl of 10 mM EGTA. C2AB, C2A, or C2B were added to each reaction as indicated in the figures. Samples were preincubated at 37 °C for 20 min followed by injection of 5 μl of 18 mM Ca^{2+} to give a final concentration of 1 mM free Ca^{2+}. Following Ca^{2+}-injection fluorescence intensity was monitored for 60 min at 37 °C using a BioTek Synergy HT plate reader equipped with 460/40 excitation and 530/25 emission filters. The maximum fluorescence signal was obtained by addition of 25 μl of *n*-dodecyl β-D-maltoside to each reaction well; samples were monitored for an additional 30 min until a stable baseline was obtained.

The fusion data were normalized by setting the initial time point to 0% and the maximal fluorescence signal in detergent to 100%. All graphs and plots were generated and analyzed using Prism 4.0 software (GraphPad, Inc.).

Co-flotation and Assembly Assays—100-μl reactions were prepared containing 50 μM C2A or C2B or 10 μM C2AB, 45 μl of either t-SNARE heterodimer, syntaxin alone, or protein-free vesicles, 2 μl of 10 mM EGTA, and reconstitution buffer in the presence or absence of 1 mM free Ca^{2+}. Components were incubated at room temperature for 30 min with shaking. Following incubation, the vesicles were mixed with 100 μl of 80% Accudenz (with or without Ca^{2+}), transferred to ultra clear centrifuge tubes, and layered with 35%, 30%, and 0% Accudenz (with or without Ca^{2+}) to form a step gradient. Gradients were centrifuged in a SW-55 rotor (55,000 rpm, 1.75 h), and 40 μl of vesicles was collected at the 0–30% interface and analyzed by SDS-PAGE and Coomassie staining or immunoblotting. Samples to be immunoblotted were transferred to nitrocellulose by the semi-dry method, nonspecific sites were blocked with 3% nonfat dry milk, and proteins were probed for with the indicated primary antibodies (diluted 1:1,000 in 1% nonfat dry milk) and a goat-anti mouse horseradish peroxidase-linked secondary antibody (diluted 1:20,000 in 1% nonfat dry milk). Blots were incubated with enhanced chemiluminescent substrate and exposed to film.

PS Binding Assays—Mutant syt 1 C2AB-glutathione *S*-transferase fusion proteins were expressed and purified as described above using glutathione-Sepharose beads, however, the protein was not eluted by thrombin cleavage. Sepharose beads containing 10 μg of bound protein were incubated with protein-free liposomes (15% PS, 29.25% PE, 55% PC, and 0.75% Rhodamine-PE) in the presence or absence of Ca^{2+} for 15 min with gentle agitation. All buffers contained 0.2 mM EGTA and Ca^{2+} concentrations were prepared from a 100 mM stock solution (Thermo Electron Corp, Beverly, MD) using WebMaxC (www.stanford.edu/~cpatton/webmaxcS.htm). Next, beads were washed three times with reconstitution buffer with the corresponding Ca^{2+} concentration. Bound liposomes were solubilized by addition of reconstitution buffer with 1% Triton X-100. The fluorescence intensity was measured using a BioTek Synergy HT plate reader equipped with 530/25 excitation and 590/35 emission filters. The resulting fluorescence was normalized to the maximum intensity as determined by nonlinear regression. The $[Ca^{2+}]_{½}$ and Hill slope for each mutant were determined by fitting the normalized data with sigmoidal dose-response curves.

Dynamic Light Scattering—Phospholipid vesicles (15% PS, 30% PE, 55% PC) were prepared by drying the phospholipids under a stream of nitrogen, subjected to vacuum for >2 h, and suspended in HEPES-buffered saline (50 mM HEPES, pH 7.4, 0.1 M NaCl, 10% glycerol, 1 mM dithiothreitol). Small unilamellar liposomes were prepared using a mini-extruder (Avanti Polar Lipids) with a 50 nm pore size membrane (Whatman). Dynamic light scattering experiments were performed on an N4 plus Submicron Particle Size Analyzer (Beckman Coulter, Inc.), with a scattering angle of 90°. Data were analyzed with PCS software. Liposomes (0.05 mM phospholipids) were mixed with either 4 μM or 10 μM protein in HEPES-buffered saline. Samples were loaded into a cuvette, and all of the experiments were thermostatically controlled at 22 °C. To determine the kinetics of vesicle aggregation, the particle size in the lipid-protein mixture was estimated at 305, 535, 765, 995, 1225, and 1455 s after the addition of 1 mM Ca^{2+} or 0.2 mM EGTA. Particle size was measured again after addition of 5 mM EGTA.

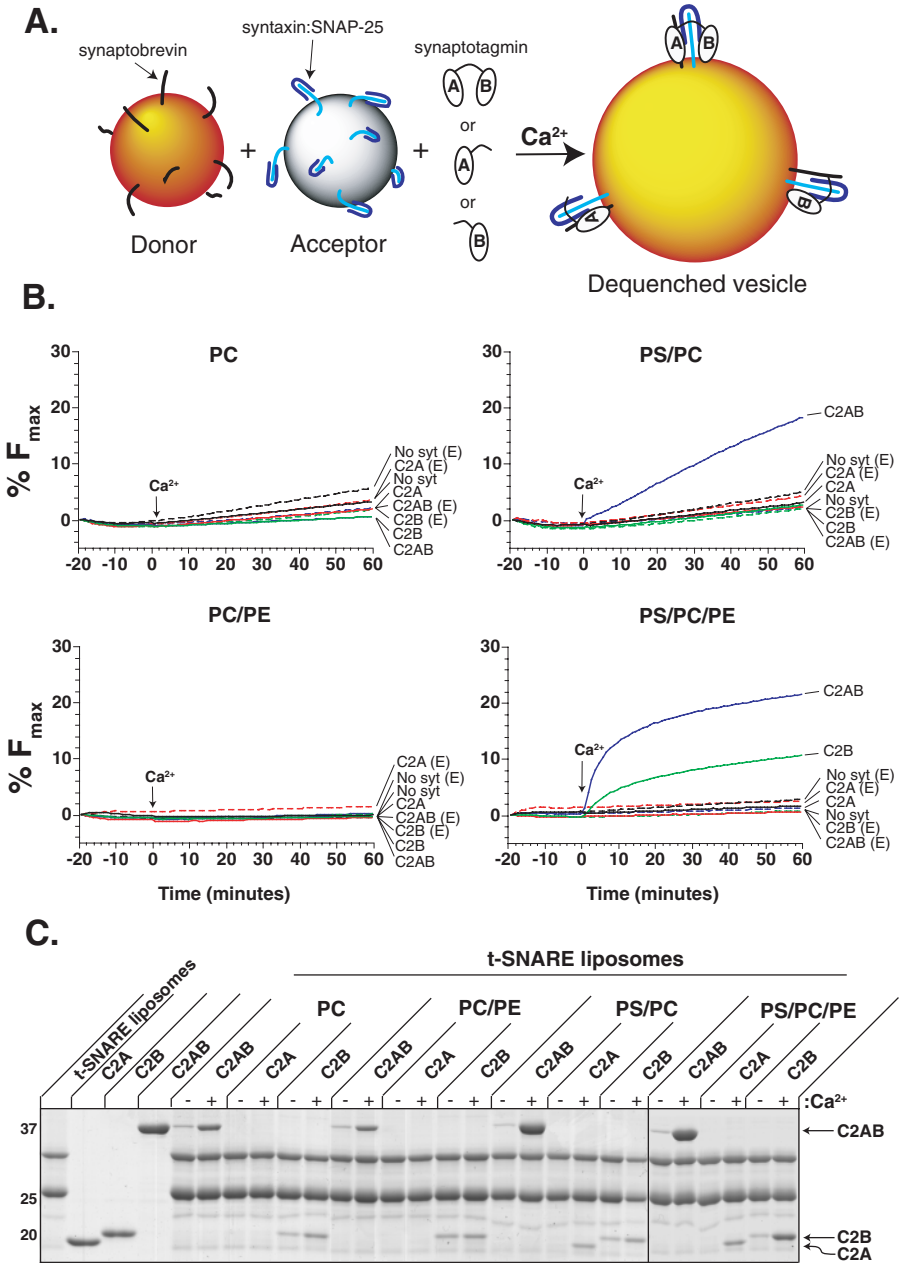

FIGURE 1. **The isolated C2B domain of syt 1 is sufficient to regulate Ca^{2+}-triggered membrane fusion.** *A*, shown is a schematic diagram depicting the components of the *in vitro* fusion assay. *B*, fusion assays were carried out using donor v-SNARE vesicles, t-SNARE acceptor vesicles, and 10 μM of the C2AB, C2A, or C2B domain of syt 1. Components were incubated together for 20 min at 37 °C in the presence of 0.2 mM EGTA, followed by the addition of Ca^{2+} (*arrow*) to give a final free concentration of 1 mM. Fluorescence intensity was measured every minute for 60 min and normalized as described under "Experimental Procedures." Reconstituted v- and t-SNARE vesicles were composed of either: 100% PC, 15%PS/85%PC, 30%PE/70%PC, or 15%PS/30%PE/55%PC. Shown are representative traces from three independent experiments. *C*, binding of each domain to t-SNARE vesicles was monitored using a co-flotation assay; t-SNARE vesicles used in the fusion assays were incubated with 10 μM C2AB, 30 μM C2A, or 30 μM C2B in the presence or absence of 1 mM Ca^{2+}. Bound material co-floated through a density gradient and was analyzed by SDS-PAGE and Coomassie Blue staining. Shown is a representative gel of three independent experiments. Note: the *line* between the PS/PC and PS/PC/PE samples indicates the data were obtained from two different gels.

Materials—Lipids were purchased from Avanti Polar Lipids (Alabaster, AL). Immunoblotting substrate and reducing agent compatible BCA kits were from Pierce-Thermo Scientific (Rockford, IL). Affinity media (Ni^{2+}-Sepharose HP and glutathione-Sepharose beads were from GE-Amersham Biosciences, Pittsburgh, PA). Accudenz was from Accurate Chemical & Scientific Corp. (Westbury, NY). All other general laboratory chemicals and supplies were from Sigma or Fisher Scientific.

RESULTS

C2B-regulated Liposome Fusion Depends on PE—Unlike experiments performed in cells, reconstituted fusion systems provide a simple means to explore the lipid requirements of Ca^{2+}-triggered fusion. Here we test alternative lipid compositions in a lipid-mixing assay in which t- and v-SNARE proteins have been reconstituted into separate vesicle populations. Donor v-SNARE vesicles containing lipids that harbor the fluorescence resonance energy transfer pair NBD and Rhodamine were incubated with excess acceptor t-SNARE vesicles that lacked the fluorescence resonance energy transfer pair. When mixed, v- and t-SNARE vesicles fuse with each other, resulting in the dilution of the fluorescence resonance energy transfer pair. Dequenching of the NBD signal is used to monitor fusion (Fig. 1*A*) (18). To test various lipid compositions, t-SNARE vesicles were prepared using either 100% PC, 15% PS/85% PC, 30% PE/70% PC, or 15% PS/30% PE/55% PC lipid mixtures. Preparation of the v-SNARE vesicles was identical to the t-SNAREs except 1.5% NBD-PE and 1.5% Rhodamine-PE were included in the lipid mixture, and unlabeled PE was adjusted to 27%.

Soluble C2AB, C2A, or C2B fragments of syt 1 were incubated with v- and t-SNARE vesicles for 20 min at 37 °C followed by injection of a Ca^{2+} bolus to give a final concentration of 1 mM (*arrow*). Consistent with previous work, PS was found to be an essential cofactor for C2AB-mediated fusion (20); vesicles composed of either 100% PC or 30% PE/70% PC did not support Ca^{2+}-triggered fusion (Fig. 1*B*, *left panels*). C2AB was able to regulate fusion between vesicles composed of 15% PS/85% PC, however, this fusion was slow, and isolated C2A and C2B were without effect, as previously reported (19, 28, 29). PE was then included in the lipid mixture of the artificial vesicles to more closely mimic the endogenous synaptic vesicle and plasma membrane

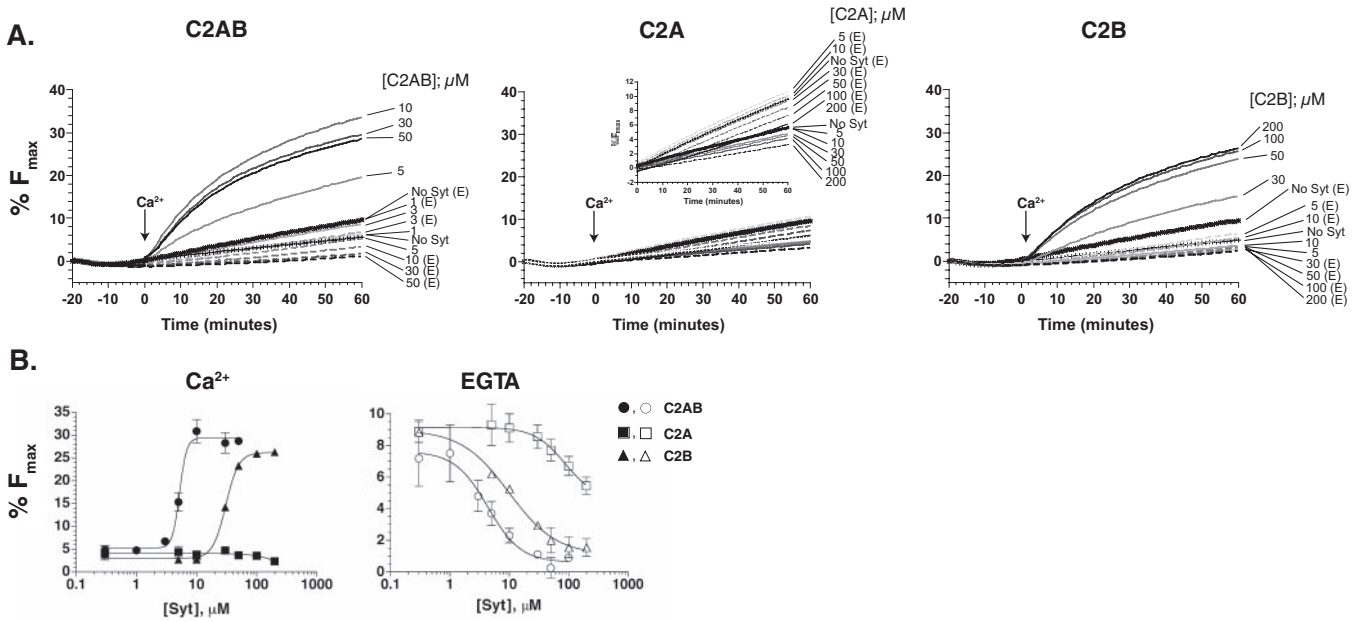

FIGURE 2. **Dose response of Ca^{2+}-triggered fusion regulated by the C2AB, C2A, or C2B domains of syt 1.** *A*, shown are representative traces ($n \geq 2$ experiments) of Ca^{2+}-triggered fusion between t- and v-SNARE vesicles as a function of C2AB, C2A, or C2B concentration. *B*, the normalized fluorescence intensity at 60 min was plotted as a function of the syt 1 domain concentration. The EC_{50} for Ca^{2+}-triggered fusion was 5.22 ± 1.1 μM and 30.6 ± 1.0 μM for C2AB and C2B, respectively. Similarly, the ability of each syt 1 domain to inhibit fusion in the presence of EGTA was plotting, and the IC_{50} was determined to be 4.34 ± 1.5 μM for C2AB, 9.8 ± 1.3 μM for C2B, and >100 μM for C2A.

lipid composition (39, 40). PE itself, in the absence of syt 1, had a slight inhibitory effect on basal SNARE-mediated fusion. In contrast, inclusion of PE markedly increased the kinetics of C2AB-regulated fusion; the initial rate of fusion, upon addition of Ca^{2+}, was increased >9-fold (Fig. 1*B*, *right panels*). Interestingly, PE also unmasked a previously unobserved regulatory activity mediated by the isolated C2B domain. C2B alone was able to clamp fusion in EGTA and to accelerate fusion in response to Ca^{2+}. To our knowledge this is the first evidence for the autonomous function of C2B during membrane fusion *in vitro* (Fig. 1*B*).

C2B Binds t-SNAREs in a Ca^{2+}-dependent Manner—In an earlier study, the interaction of isolated syt 1 domains, with reconstituted full-length t-SNARE heterodimer, was addressed using a co-flotation assay (19). C2AB exhibited the greatest degree of t-SNARE-binding activity; isolated C2B bound t-SNAREs to a lesser degree, and binding of isolated C2A was not detected. In light of the new observation that PE enables isolated C2B to regulate Ca^{2+}-triggered SNARE-mediated fusion, we re-examined the ability of C2B to bind to t-SNARE vesicles that did, and did not, harbor PE. These experiments were carried out to determine if C2B binds directly to PE, influences C2B-t-SNARE interactions, or affects the fusion reaction via an indirect mechanism (detailed further below).

We note that syt 1 C2AB can bind to vesicles via interactions with either t-SNAREs or PS (19). Therefore, to selectively examine t-SNARE-binding activity, these experiments included vesicles that harbored t-SNAREs but lacked PS. Vesicles were incubated with either 10 μM C2AB, or 50 μM C2A or C2B, and floated through a density gradient (Fig. 1*C*). C2AB and isolated C2B, but not the isolated C2A domain, bound to PS-free t-SNARE vesicles in a Ca^{2+}-dependent manner. Protein-free vesicles, for each lipid mixture, were run in parallel; C2AB, C2A, and C2B co-floated with vesicles that contained PS in response to Ca^{2+}, consistent with the PS-binding activity of each fragment. Importantly, C2AB, C2A, or C2B failed to co-float with vesicles that lacked both t-SNARE heterodimers and anionic phospholipids (*i.e.* PS, data not shown); thus, none of these syt 1 fragments exhibited detectable PE-binding activity. These data confirm that, in our co-flotation assay, C2AB and isolated C2B, but not isolated C2A, assemble into readily detectable complexes with t-SNAREs via interactions that are strengthen by Ca^{2+} (30). Given the nature of the co-sedimentation assay, we cannot rule out a weak interaction of the isolated C2A domain with SNAREs, and we reiterate the finding that, when tethered to C2B, C2A acts to increase the affinity of syt 1 for syntaxin and SNAP-25 (11, 19, 30, 41).

The Isolated C2B Domain Exhibits Both Stimulatory and Fusion-clamping Activities—Titration experiments were performed to determine if C2A or C2B could give rise to similar levels of fusion as C2AB. In response to Ca^{2+}, C2B drove fusion almost as efficiently as C2AB, but the EC_{50} for the isolated C2 domain (EC_{50} = 30.6 ± 1.0 μM) was 6-fold greater than for the tethered C2 domain fragment of syt (EC_{50} = 5.2 ± 1.1 μM). In contrast, even at the highest concentration of C2A tested, stimulation was not observed (Fig. 2*A*). We conclude that, although C2B is necessary and sufficient to regulate fusion, a tethered, adjacent C2A enhances the function of C2B.

In addition to Ca^{2+}-stimulated fusion activity, the ability of each domain to inhibit basal SNARE-mediated fusion in EGTA was also analyzed. The IC_{50} values for C2AB, C2A, and C2B were 4.3 ± 1.5 μM, > 100 μM, and 9.8 ± 1.3 μM, respectively (Fig. 2*B*). So, although high concentrations of isolated C2A were ineffective at regulating Ca^{2+}-triggered fusion, this domain did exhibit a slight ability to clamp SNARE-mediated fusion in the presence of EGTA, but only at concentrations

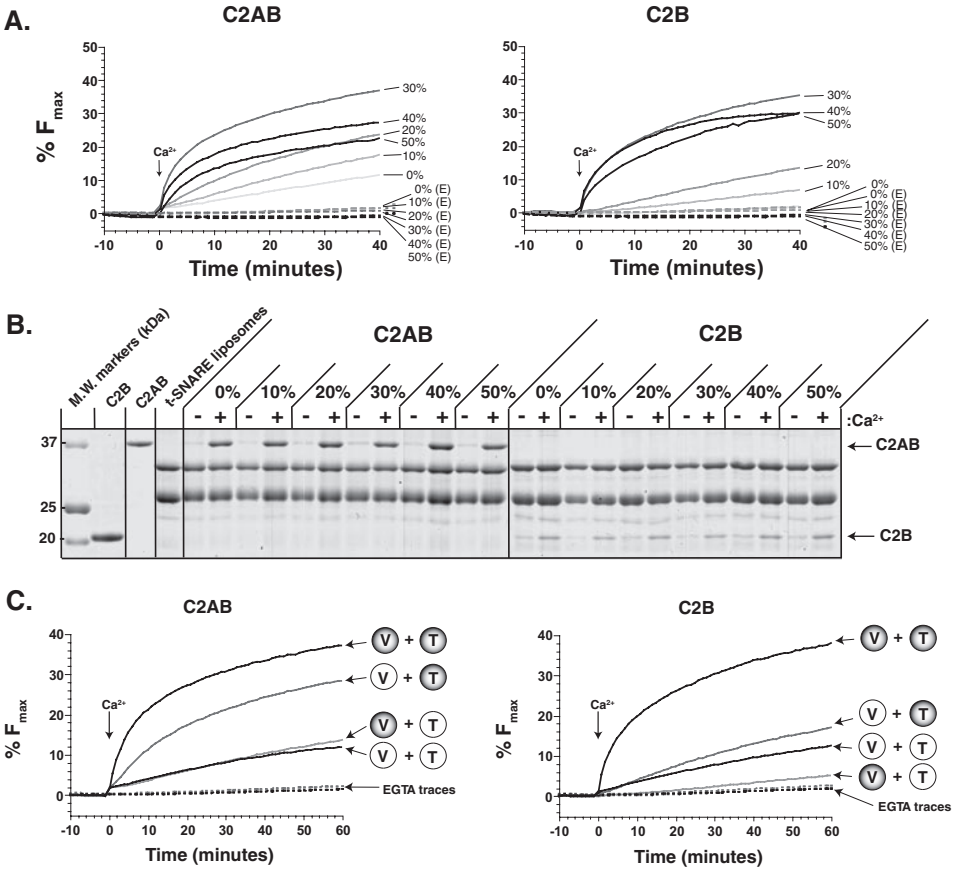

FIGURE 3. **Characterization of PE in the *in vitro* fusion assay.** *A*, PS/PC/PE t- and v-SNARE vesicles were prepared as described, with either 0, 10, 20, 30, 40, or 50% PE, incubated with either 10 μM C2AB or 50 μM C2B, and analyzed in the fusion assay. *B*, the ability of each domain to bind t-SNAREs was monitored by flotation assays. PS-free vesicles containing 0, 10, 20, 30, 40, 50% PE were incubated with 10 μM C2AB or 50 μM C2B and floated through a density gradient in the presence or absence of 1 mM Ca^{2+}. Vesicles were collected from the top of the gradient, separated by SDS-PAGE, and stained with Coomassie Blue. Shown are representative fusion traces, and a Coomassie-stained gel, from three separate experiments. *C*, shown are representative fusion traces ($n = 2$) in which 10 μM C2AB (*left*) or 50 μM C2B (*right*) were incubated with t- and v-SNARE vesicles with (*shaded*) and without 30% PE (*clear*).

$\geq$30 μM. This finding suggests that, in the absence of Ca^{2+}, C2A might weakly interact with t-SNAREs causing an inhibition of basal SNARE-mediated fusion. Interestingly, the clamping activity of C2B was reduced only 2-fold as compared with C2AB. This is in marked contrast to the Ca^{2+}-triggered activity of syt, where C2AB was 6-fold more effective than C2B. Therefore, although isolated C2B can clamp fusion under resting conditions and accelerate fusion in response to Ca^{2+}, an adjacent C2A domain facilitates both of these activities, especially the activation of fusion.

PE Requirements for Enhanced Membrane Fusion—The ability of isolated C2B to regulate fusion is strictly dependent on the presence of PE in the vesicles. To further characterize this observation, PE was titrated from 0 to 50% of the total lipid (Fig. 3*A*). As the percentage of PE was increased, C2AB and C2B displayed dose-dependent increases in initial rate and fusion efficiency. C2AB and C2B functioned optimally at 30% PE, but activity began to diminish at higher concentrations (supplemental Fig. S1). The decreased efficiency of C2AB and C2B at high PE concentrations might be explained by the cone-like characteristics of PE, which could alter the structure of the t- and v-SNARE vesicles due to its ability to form inverted hexagonal arrays and micelles (42).

To confirm our observation that PE does not affect the ability of C2AB or C2B to bind t-SNAREs (Fig. 1), additional flotation assays were performed. PS-free t-SNARE vesicles containing 0, 10, 20, 30, 40, and 50% PE were incubated with 10 μM C2AB or 50 μM C2B in the absence or presence of Ca^{2+}. Both C2AB and C2B bound t-SNAREs equally well at all PE concentrations tested (Fig. 3*B*). Protein-free vesicles were run in parallel, and no significant binding of either C2AB or C2B was detected (data not shown). Together with the data from Fig. 1, these results suggest that PE might affect a step immediately preceding fusion but after C2AB or C2B have bound to t-SNAREs.

To determine whether PE exerts its effect on C2B-regulated membrane fusion by acting at either the t- or v-SNARE membrane, experiments were carried out in which PE was omitted from each population of vesicles. When PE was omitted from the v-SNARE membrane, C2AB retained ~74% of its maximal efficiency. In contrast, when PE was omitted from the t-SNARE vesicles alone, or both v- and t-SNARE vesicles together, only ~32% of the maximal efficiency was retained (Fig. 3*C*). Thus, PE in the t-SNARE membrane largely mediates the enhanced rate and efficiency of fusion in the presence of Ca^{2+} and C2AB. This finding is consistent with previous studies indicating that syt acts on the target membrane to regulate fusion (7, 17).

Similar experiments were carried out for the isolated C2B domain, but with different results. Omission of PE from either the v- or t-SNARE vesicle alone resulted in a marked decrease in the rate and efficiency of C2B-regulated fusion; in either case, only ~30% of the maximal extent of fusion persisted (Fig. 3*C*). The retention of some C2B activity, when PE is present in either the t- or v-SNARE membranes, indicates that PE is still able to enhance Ca^{2+}-triggered fusion. However, unlike C2AB, optimal fusion activity of C2B requires PE in both t- and v-SNARE vesicle populations.

The Isolated C2B Domain of syt 1 Drives Assembly of SNAP-25 onto Membrane-embedded Syntaxin—A recent study demonstrated that C2AB drives assembly of functional t-SNARE heterodimers (20). To test whether the isolated C2B domain exhibits this activity, C2B was incubated with soluble SNAP-25 and membrane-embedded syntaxin in either EGTA

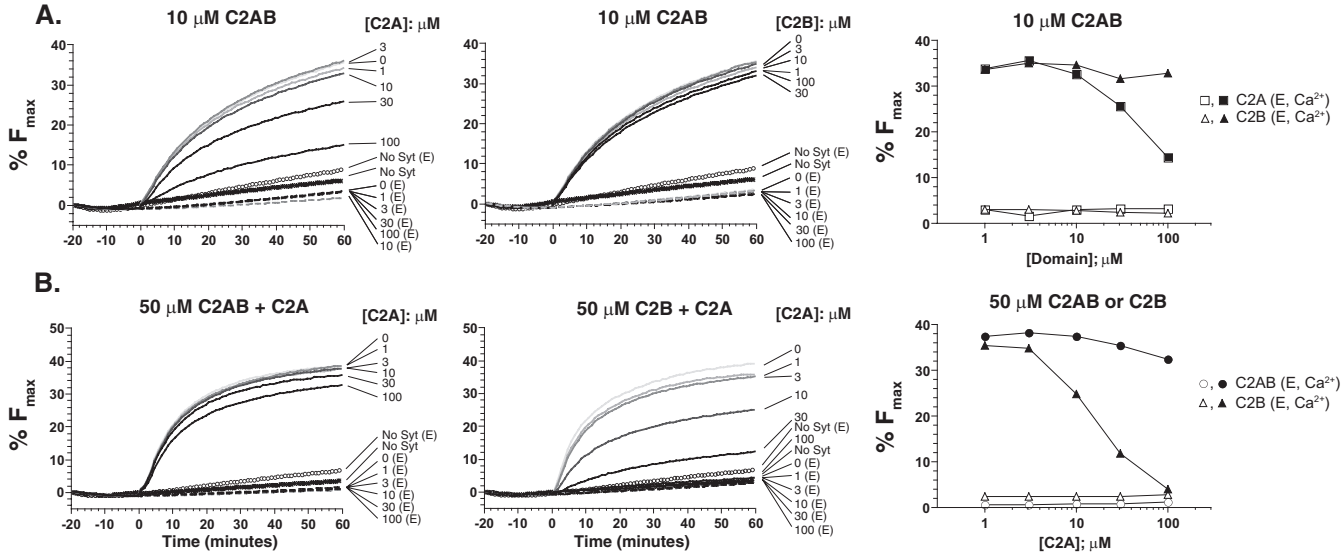

FIGURE 4. **The isolated C2A domain of syt 1 inhibits C2B-regulated fusion.** *A*, representative traces of two separate experiments demonstrating the ability of C2A or C2B to inhibit C2AB regulated vesicle fusion. Ca^{2+}-triggered fusion assays were performed with 10 μM C2AB and increasing concentrations of either C2A (*left*) or C2B (*center*), and the $\%F_{max}$ was plotted as a function of the isolated C2 domain concentration (*right*). These data indicate that high molar ratios of isolated C2A, but not isolated C2B, inhibit C2AB-regulated fusion. *B*, representative traces demonstrating the ability of C2A to inhibit C2AB or C2B-regulated fusion. The concentration of C2AB (*left*) and C2B (*center*) was maintained at 50 μM to observe robust C2B-regulated fusion. The efficacy of C2A-mediated inhibition was determined by plotting the $\%F_{max}$ for each domain as a function of C2A concentration (*right*).

or Ca^{2+} (supplemental Fig. S2). Under our assay conditions, little binding of SNAP-25 to membrane-embedded syntaxin was observed (18, 20). However, addition of 50 μM C2AB or C2B drove the assembly of SNAP-25 onto reconstituted syntaxin in a Ca^{2+}-dependent manner (supplemental Fig. S2, *B* and *C*); hence, isolated C2B does "work" on SNARE proteins. In contrast, the isolated C2A domain (50 μM) was unable to assemble SNAP-25 onto syntaxin.

Isolated C2A Inhibits C2AB- and C2B-regulated Fusion—To further characterize the function of C2A and C2B, each domain was titrated against C2AB in the reconstituted fusion assay. When the concentration of C2AB was held constant at 10 μM, and increasing concentrations of either C2A or C2B were added, C2A, but not C2B, inhibited fusion (Fig. 4*A*). Next, we tested the efficacy of C2A against either C2AB- or C2B-regulated fusion. When C2A was titrated against 50 μM C2AB very little inhibition was observed (~15% at 100 μM C2A). In contrast, when C2A was titrated against 50 μM C2B, 90% of fusion was blocked by 100 μM C2A (Fig. 4*B*). These data suggest C2A might compete for binding sites on t-SNARE vesicle; however, preliminary experiments indicate that C2A cannot displace C2B from the fusion complex (data not shown). These findings raise the possibility that C2A co-assembles into fusion complexes to reduce their activity. Further biochemical characterization is needed to test this hypothesis.

Scanning Alanine Mutagenesis of the Cytosolic Domain of syt 1—We next carried out scanning alanine mutagenesis to identify surfaces of syt 1 that may participate in regulated membrane fusion. Increased ionic strength disrupts syt 1-t-SNARE interactions (11, 43); therefore, we limited our mutations to charged residues that would affect electrostatic interactions. Also, given the newly discovered autonomous function of C2B, most of our mutations were focused on this domain. In total, 42 point mutants (10 in C2A and 32 in C2B) and 7 multiple mutant forms of C2AB were generated. These mutants were screened for function in the lipid mixing assay. We note that previous studies have suggested the sensitivity of the *in vitro* lipid mixing assay is relatively low. For instance, mutations within the linker of syt 1 yielded marked effects on secretion in PC12 cells, but had only modest effects when later analyzed in the reconstituted fusion assay (8, 11). The relative low sensitivity of the assay assures that only mutants with strong effects will be identified.

For each mutant the $\%F_{max}$ at 60 min was normalized to data obtained using wild-type (wt) C2AB (Fig. 5*A*). In most cases no apparent change in Ca^{2+}-triggered fusion or clamping activity was observed. However, several mutants could be grouped based on their distinct Ca^{2+}-dependent and independent activities. These groups were visualized based on the percentage of wt fusion retained for each mutant following the addition of Ca^{2+} and plotted *versus* its change in clamping activity (fusion in EGTA) (Fig. 5*B*). From this analysis the mutants could be divided into four distinct populations.

The first set of mutations, T328 and E341, resulted in ~20% loss of Ca^{2+}-triggered fusion activity but no significant loss in Ca^{2+}-independent clamping activity. These mutants bind t-SNARES and PS in a Ca^{2+}-dependent manner (Figs. 6 and 7), indicating that they are not dramatically misfolded. The extent of t-SNARE binding was actually enhanced in both EGTA and Ca^{2+} conditions; however, the relative increase in t-SNARE binding in response to Ca^{2+} was lower. The T328A and E341A mutants had a reduced ability to drive the assembly of SNAP-25 onto membrane-embedded syntaxin (supplemental Fig. S3), suggesting defects in their ability to drive structural transitions in SNARE proteins. We note that Sr^{2+} triggers the binding of syt 1 to t-SNAREs but is unable to activate fusion (8). The ability of Sr^{2+} to uncouple C2AB·t-SNARE binding from regulated fusion is somewhat similar to the effect of the T328A and

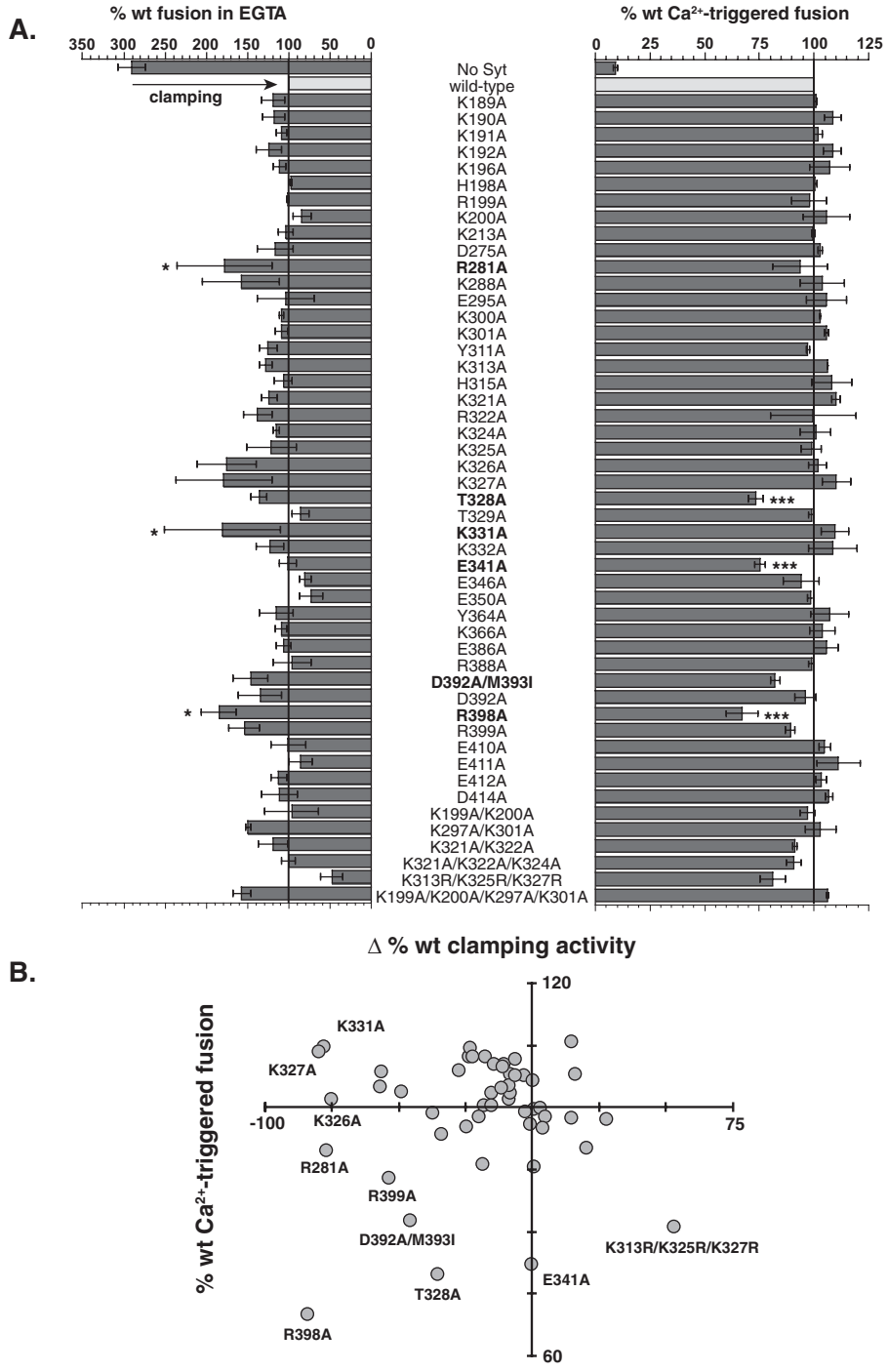

FIGURE 5. **Scanning alanine mutagenesis reveals distinct regions of syt 1 that are important for Ca^{2+}-triggered fusion.** *A*, the $\%F_{max}$ at 60 min was determined and normalized to the wt activity and plotted for each mutant. The histogram shows the extent of Ca^{2+}-stimulated (*right*) and Ca^{2+}-independent (*left*) fusion for each mutant relative to wt C2AB (*gray*). The mean ± S.E. for each mutant was generated from ≥3 independent experiments. Significance was determined by one-way analysis of variance ($* = p < 0.05$, $** = p < 0.01$, and $*** = p < 0.001$). *B*, to determine if there was a correlation between a mutant's ability to activate Ca^{2+}-triggered fusion or their ability to clamp fusion in EGTA, these values were plotted against each other for each mutant. Select mutants are labeled to highlight their location on the plot.

E341A mutations; these mutants also appear to dissociate t-SNARE-binding activity from the ability of syt to drive folding of t-SNAREs and to regulate membrane fusion.

A second set of mutations, D392A/M393I, R398A, and R399A, again reduced Ca^{2+}-triggered fusion by 20–30% but also had a concomitant 30–40% reduction in clamping activity. Further analysis of the R398A mutant revealed substantial decreases in t-SNARE-binding activity (Fig. 6) and SNAP-25-syntaxin assembly activity (supplemental Fig. S3). However, the R398A mutant still exhibits robust PS-binding activity, indicating that this mutant is correctly folded (Fig. 7). In addition, R398A retains the vesicle aggregation properties of wt C2AB (supplemental Fig. S4). Together, these data strongly indicate that residue 398, on the opposite end of this domain as the Ca^{2+}/membrane-binding loops (see Fig. 8), directly interacts with t-SNAREs to regulate fusion. This is a particularly interesting finding, because this region of C2B has not been previously implicated in interactions with t-SNAREs nor any other biochemical function of syt.

A third set of mutations (*e.g.* K326A, K327A, and K331A) displayed diminished clamping activity but did not exhibit dramatic changes in their ability to stimulate fusion in response to Ca^{2+}. Finally, a fourth mutant, K313R/K325R/K327R, appeared to clamp fusion more effectively than wt C2AB, consistent with a slight increase in its t-SNARE binding (Fig. 6). We also note that this mutant exhibited a higher degree of cooperativity for binding to PS/PE/PC vesicles (Fig. 7; note that the cooperativity values reported in Fig. 7*B* are lower than in previous reports (11, 34) due to inclusion of PE in the vesicles and the use of lower amounts of PS). Together with T328A and E341A, these data demonstrate that the Ca^{2+}-dependent stimulatory function of syt 1 can be uncoupled from its clamping activity in the absence of Ca^{2+}.

DISCUSSION

Reconstituted systems can be used to recapitulate the function of cellular machines in a way that makes it possible to directly ascertain the function of each component in a direct and step-by-step manner. It is critical for reconstituted systems to converge, functionally, with native systems. A goal of the current study was to improve a model system that is used to study Ca^{2+}-triggered membrane fusion based on proteins that mediate SV

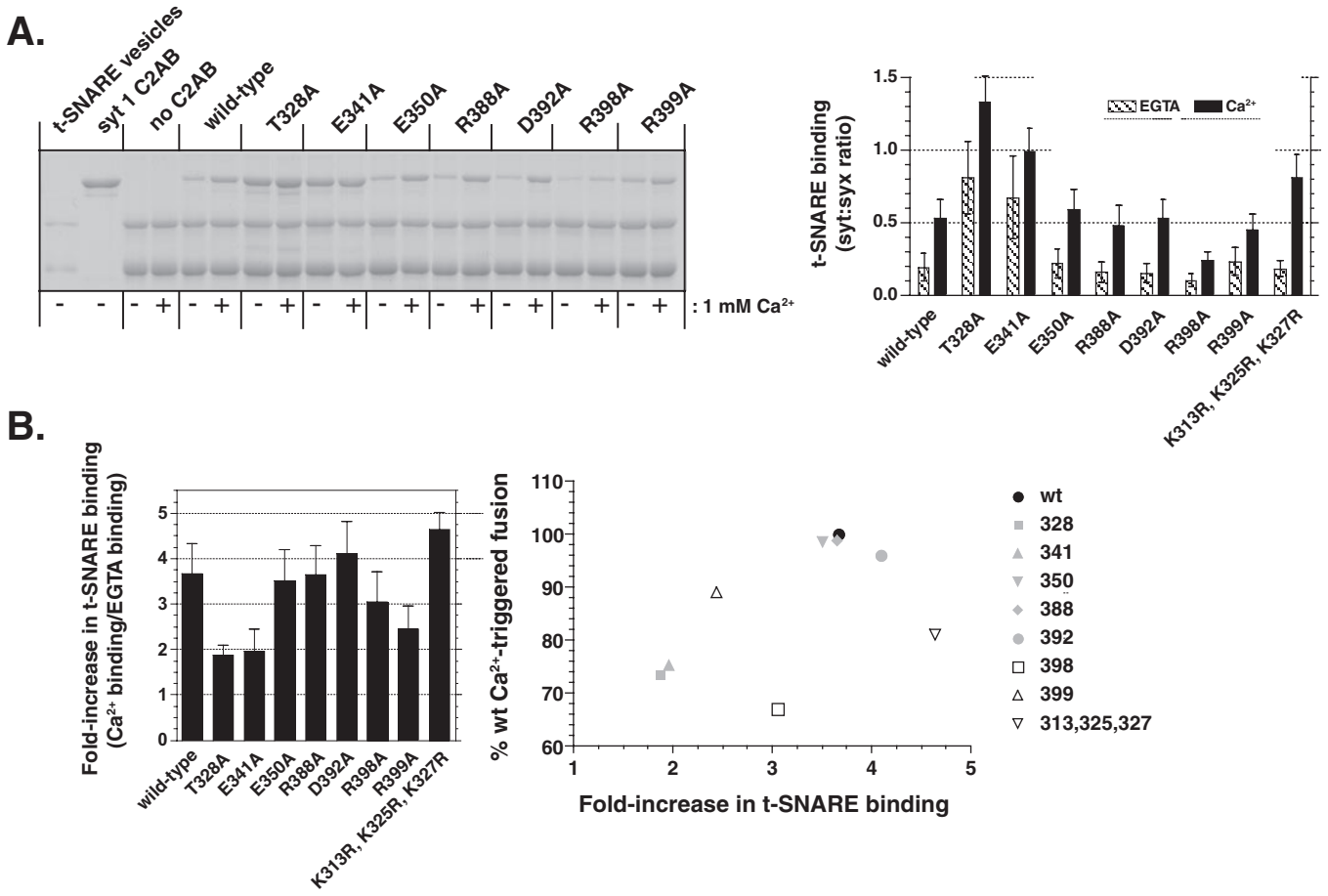

FIGURE 6. **The R398A mutation inhibits the t-SNARE-binding activity of syt 1 in both the absence and presence of Ca^{2+}.** *A*, a representative t-SNARE binding experiment of selected mutants ($n = 4$) is shown. PS-free t-SNARE vesicles were incubated with 10 μM of each mutant in the presence or absence of Ca^{2+}, floated through a density gradient, and analyzed by SDS-PAGE. The optical density of the syt and syntaxin bands was measured, and the ratio was used to determine the extent of binding (*right*). *B*, the -fold increase in syt 1 C2AB binding to t-SNAREs in response to Ca^{2+} was calculated for each mutant (*left panel*). These data are plotted against the relative extent of fusion (normalized to the amount of fusion observed using wt protein (*right panel*)).

exocytosis in neurons. More specifically, to better mimic the lipid composition that occurs *in vivo*, with an emphasis on PE. PE composes ~30–36% of the total phospholipid content of the plasma and SV membranes (39, 40) and is the only major phospholipid missing from previous fusion assays (8, 17–19).

In this study, we carried out the first systematic analysis of PE in the reconstituted Ca^{2+}-triggered fusion assay. Addition of PE to our artificial vesicles enhanced the rate and efficiency of Ca^{2+}·C2AB-regulated fusion. This effect was optimal at ~30% PE, suggesting that syt 1 may be tuned to operate at physiological levels of this lipid. Moreover, inclusion of PE resulted in a surprising and novel finding: under this condition, the isolated C2B domain of syt 1 was capable of facilitating fusion in response to Ca^{2+}. The enrichment of PE in the inner leaflet of the plasma membrane (44) and its cone shape, which is conducive to membrane bending, may lower the free energy required to form a membrane stalk during the initial steps of vesicle fusion (45). The finding that PE enhances C2AB and C2B function, without altering their abilities to engage t-SNAREs (Fig. 3), is consistent with this model; C2B is able to regulate SNARE-mediated fusion in the presence of PE due to a lowered energy barrier.

The autonomous function of C2B reported here would seem to contradict recent studies, in which C2B alone was not able to regulate Ca^{2+}-triggered fusion (19, 28, 29). Three significant differences in assay conditions between the current study and previous reports readily explain the apparent discrepancy. The first study, which characterized the effect of C2AB and C2A plus C2B in the fusion assay, did not include PE in the vesicles (19). Hence, C2B was without effect (Fig. 1). Second, simultaneous addition of equal molar amounts of both isolated domains, C2A plus C2B, results in an apparent lack of function, even in the presence of PE, due to the ability of C2A to block C2B-mediated stimulation (Fig. 4*B*). Third, the concentration of C2B required to yield fusion is ~6-fold greater than for C2AB (Fig. 2*B*). Therefore, C2B-regulated fusion will not be detected if relatively low concentrations of C2B are tested (*i.e.* < 10 μM) (28, 29).

The C2A domain has distinctly different effects depending on how it is partnered with C2B. When tethered to C2B, C2A plays a positive role to enhance the activity of C2AB as compared with isolated C2B. However, when the linker connecting the two domains is severed, we found that not only is the synergy between these C2 domains lost but that C2A, in *trans*, now inhibits the action of C2B. Thus far, competition experiments with C2AB and C2B have not revealed C2A-mediated displacement from the fusion complex, raising the possibility that C2A co-assembles with the fusion machinery to disrupt function.

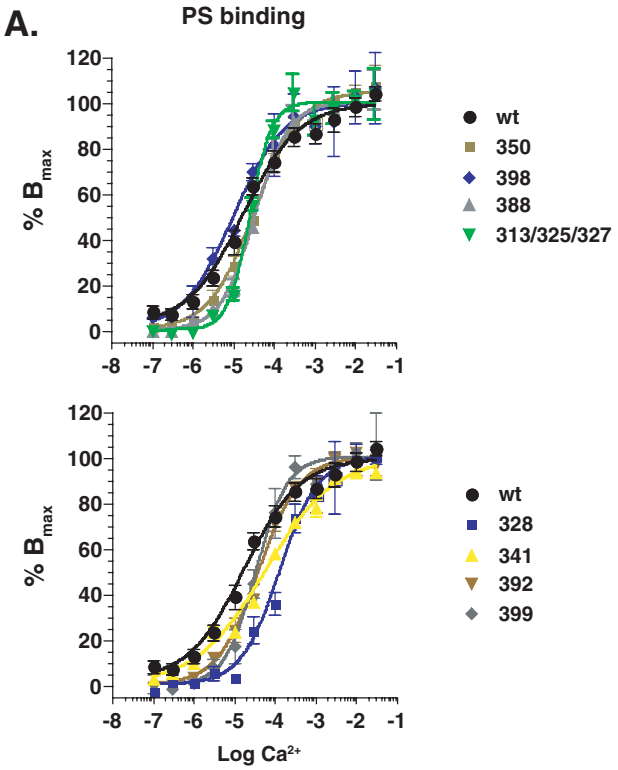

B.

Protein	Hill Slope	$[Ca^{2+}]_{1/2}$ (μM)
wild-type	0.64 ± 0.10	18.4 ± 6.8
T328A	0.91 ± 0.19	136.8 ± 34.3
E341A	0.51 ± 0.06	60.5 ± 14.1
E350A	0.78 ± 0.09	34.7 ± 5.7
R388A	1.04 ± 0.14	35.6 ± 5.3
D392A	0.86 ± 0.10	41.8 ± 6.6
R398A	0.69 ± 0.22	10.7 ± 7.0
R399A	1.14 ± 0.23	36.3 ± 7.6
K313R, K325R, K327R	1.63 ± 0.28	26.8 ± 3.3

FIGURE 7. **Ca^{2+}-dependent PS-binding activity of syt 1 C2AB mutants.** *A*, the PS-binding activity of wt and several mutant forms of syt 1 C2AB was measured using a glutathione *S*-transferase pulldown assay and plotted as a function of Ca^{2+} concentration. Mutants were grouped based on their relative changes in $[Ca^{2+}]_{1/2}$. *B*, table summarizing the Hill slope and $[Ca^{2+}]_{1/2}$ for each mutant tested.

Further biochemical/biophysical experiments will be required to discern the exact mechanism of C2A-mediated inhibition. Regardless of the mechanism of inhibition by C2A, these data provide additional support for the idea that the tandem C2 domains of syt 1 somehow interact with one another, in the context of the intact cytosolic domain of the protein (37), to enhance the function of syt during fusion. These findings are consistent with previously reported cooperative interactions between C2A and C2B, in terms of PS- and t-SNARE-binding activity (6, 11, 19, 30).

A mechanistic understanding of how C2B regulates membrane fusion will require detailed information regarding the interaction of this domain with SNARE proteins. A handful of recent studies have sought to develop models of the syt 1·SNARE complex, but a coherent view of this complex has not yet emerged (12, 31, 34). Indeed, contradictions regarding the gross mapping data abound (*e.g.* Refs. 32, 33 *versus* Ref. 46).

To gain new insight into this question, we analyzed C2AB using scanning alanine mutagenesis to search for residues that might regulate fusion via forming contacts with t-SNAREs. Given the findings detailed above, we focused most of our mutations on the C2B domain. We chose to substitute charged residues on the surface of C2B (*e.g.* arginine, lysine, aspartate, and glutamate), because prevailing evidence indicates C2AB binds t-SNARE through electrostatic interactions (11, 43). The majority of mutations resulted in protein with no apparent change in activity when screened in the fusion assay; however, four separate groupings emerged (Fig. 5*B*).

The first group of mutations, T328A and E341A, displayed a loss of Ca^{2+}-triggered fusion activity without a significant loss in Ca^{2+}-independent clamping ability. Analysis of the protein structure of C2B indicates that Thr-328 and Glu-341 are in close proximity and might interact with each other (Fig. 8*B*). These two residues are highly conserved among C2 domains from the syt family, as well as C2 domains found in a variety of additional proteins (47). Biochemically, these mutants displayed an increase in t-SNARE binding and a diminished ability to assemble SNAP-25 onto syntaxin. Hence, these mutations appear to perturb the ability of C2AB to drive structural changes in t-SNAREs without disrupting binding *per se*.

The second group of mutations resulted in a concomitant loss of Ca^{2+}-triggered fusion and clamping activity (D392A/M393I, R398A, and R399A (Fig. 8*D*)). Interestingly, R398A emerged as a mutation that might provide novel insight into the interactions between C2AB and t-SNAREs. This mutant exhibited losses in t-SNARE binding and assembly activity, but retained robust PS-binding activity (Fig. 7), indicating that it was correctly folded. In addition, the R398A mutant also retains the ability to aggregate vesicles (supplemental Fig. S4). The observation that Arg-398 lies on the opposite "end" of C2B from the Ca^{2+}/membrane-binding loops indicates that syt 1 might possess distinct t-SNARE and membrane-binding interfaces (Fig. 8, *E* and *F*). This does not necessarily contradict previous models, which suggested that regions adjacent to the membrane penetration loops of C2AB interact with t-SNAREs (12, 34). In the case of the K366A mutation in C2B (34), the region lies roughly within the t-SNARE interaction "plane" described below (Fig. 8*A*). The finding that some of these mutations affect the activity of the adjacent C2B domain complicates interpretation of the effects of mutants in C2A (34). Finally, it should also be noted that syt 1 C2AB might engage individual, isolated t-SNAREs (which were used in most of the previous studies) in a manner that is distinct from the reconstituted t-SNARE heterodimers studied here.

The third group of mutations (*i.e.* R281A, K326A, K327A, and K331A) appears to diminish Ca^{2+}-independent clamping ability of without greatly affecting Ca^{2+}-triggered fusion activity. In contrast, the fourth group had no significant change in Ca^{2+}-triggered fusion activity but exhibited enhanced clamping activity (*i.e.* K313R/K325R/K327R and E350A). Together, these findings indicate that the ability of syt 1 to inhibit SNARE function in EGTA can be separated, via mutations, from the ability of syt 1 to stimulate fusion in the presence of Ca^{2+}. Thus, this analysis has provided a useful panel of mutant syts for cell-

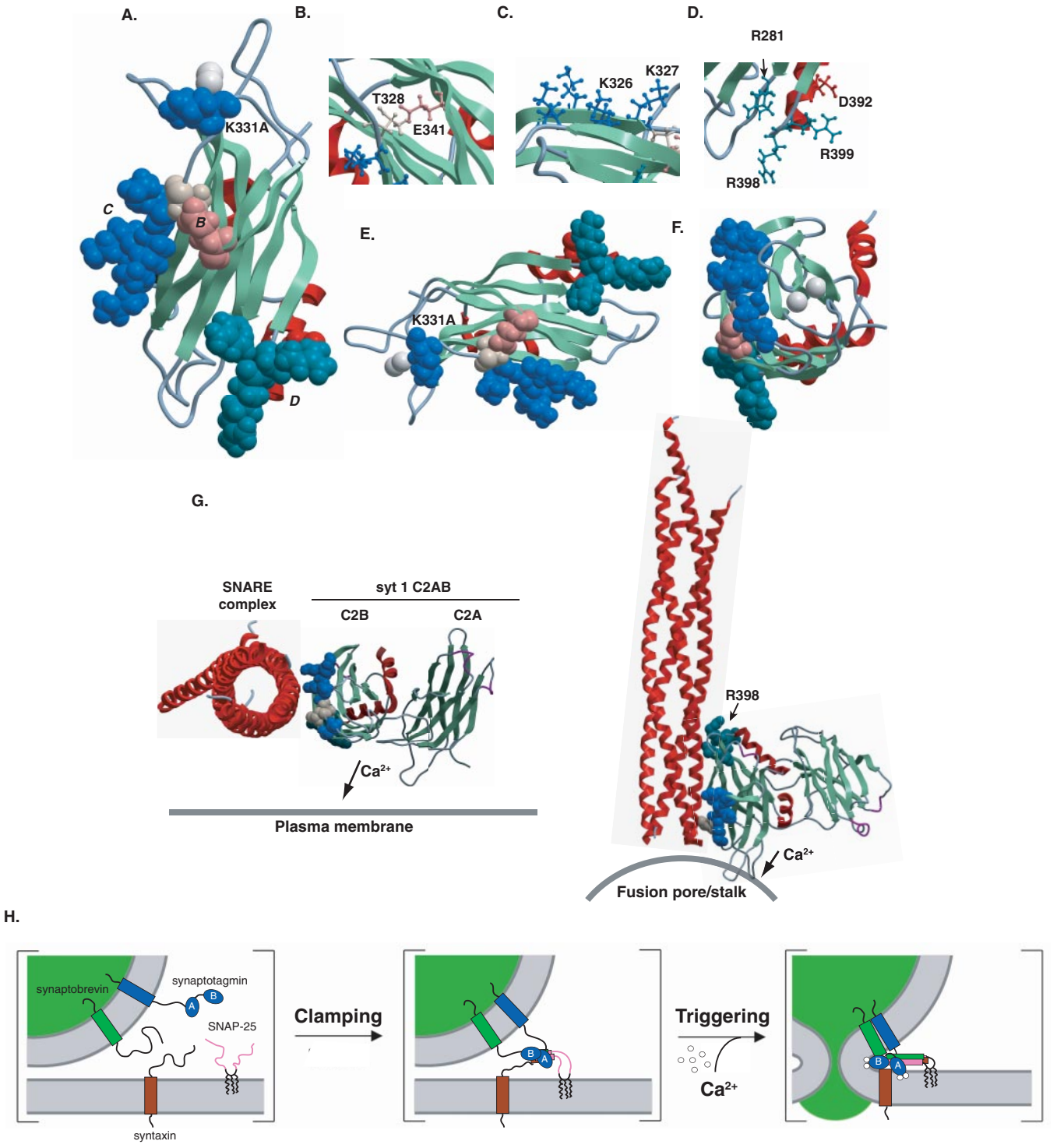

FIGURE 8. **A model of the syt 1·SNARE·membrane complex showing the surfaces of C2B proposed to interact with t-SNAREs and membranes.** *A*, shown is the NMR structure of the syt 1 C2B domain (PDB 1K5W) with Ca^{2+} ions modeled as *white spheres*. The substituted residues in the mutants that displayed decreased Ca^{2+}-triggered fusion activity are highlighted as *stick structures*. *B*, close up of residues Thr-328 (*cream*) and Glu-341 (*tan*). *C*, close up of residues Lys-326 and Lys-327 (*blue*). *D*, close up of residues Asp-392 (*red*), Arg-398, Arg-399, and Arg-281 (*aqua*). *E*, a "lateral" view of the C2B domain modeled with space-filled side chains. *F*, an "axial" view of the C2B domain from the Ca^{2+}-binding loops modeled with space-filled side chains to emphasize the alignment of the mutations on one face of C2B. *G*, a proposed model for C2AB interactions with the SNARE complex (*red*) during membrane fusion. In the absence of Ca^{2+}, C2AB initiates contact with t-SNAREs via the C2B domain through the polybasic region, and Arg-398. Influx of Ca^{2+} tightens the interaction between C2AB and the SNARE complex while the Ca^{2+}-binding loops of C2B penetrate into the fusion stalk and the Ca^{2+}-binding loops of C2A penetrate the plasma membrane. All structural images were created using ICM BrowserPro (Molsoft, La Jolla, CA) and Adobe Illustrator CS. *H*, a functional model of syt during the initial stages of SNARE assembly and following the Ca^{2+} trigger.

based functional analysis. Structurally, these findings argue for distinct modes of binding under resting and stimulating conditions; one to clamp and one to trigger fusion (17).

Whether interactions between multiple contact points between C2B and t-SNAREs occur simultaneously, or in an ordered progression remains unknown. As noted above, several

mutations in this study appear to selectively affect the Ca^{2+}-independent function of C2AB (*i.e.* R281A, K326A, K327A, and K331A), whereas, others display defects that are limited to its Ca^{2+}-dependent activity (*i.e.* T328A and E341A) (Fig. 7*A*). Indeed, previous studies have demonstrated the importance of the polylysine motif in t-SNARE binding (11) and syt function *in vivo* (26). The protein structure of C2B reveals that Arg-398, the polybasic region, Thr-328, and Glu-341 lie on one face of the domain (Fig. 8*F*) suggesting that an extended surface of C2B might be critical for t-SNARE recognition. In order for these residues to bind t-SNAREs, the C2B domain would need to align roughly parallel with the helical bundle (Fig. 8*G*). Interestingly, when the mutations are modeled on the structure of human apo-syt 1 (37), the Ca^{2+}-binding loops of C2B point toward the putative fusion stalk while the Ca^{2+}-binding loops of C2A are oriented toward the plasma membrane (Fig. 8*G*).

From the data reported here, we propose a new mechanism by which syt 1 binds to t-SNAREs via two distinct modes of interaction. Early in the assembly pathway, Ca^{2+}-independent interactions mediated by Arg-281, the polylysine regions, Lys-331, and Arg-398 might clamp SNARE-complex assembly and arrest fusion (17). Following Ca^{2+} influx, syt 1 penetrates membranes and drives final assembly of the SNARE complex, or changes the orientation of the fully assembled SNARE complex relative to the plane of the lipid bilayer, to trigger the opening and dilation of fusion pores (48). Regardless of the state of the SNARE complex, Ca^{2+}-triggered fusion seems to be regulated through direct interactions, or protein transitions, involving Thr-328, Glu-341, Arg-398, and the polybasic motif of syt 1.

In summary, we have demonstrated that inclusion of PE into SNARE-bearing vesicles results in two dramatic effects. First, PE enhances the initial rate of C2AB-regulated Ca^{2+}-triggered fusion by 9-fold. Second, PE unmasked the previously unobserved autonomous functions of the isolated C2B domain of syt 1. In the presence of PE, the isolated C2B domain, but not C2A domain, retains much of the regulatory activity of the intact cytosolic domain of the protein, including its ability to clamp SNARE-mediated fusion prior to the Ca^{2+} signal.

In addition, scanning alanine mutagenesis analysis of syt 1 C2AB revealed several point mutations within the C2B domain that dissociate the Ca^{2+}-independent clamping and Ca^{2+}-dependent stimulatory activities of the protein. Interestingly, the mutations that decreased syt 1 regulated fusion activity lie on one face of the C2B domain, suggesting syt 1 interacts with SNAREs via an extended binding surface. Hence, the data described here indicate it will be crucial to direct attention to previously unappreciated surfaces on the C2B domain of syt 1. Next, it will be important to determine whether the mutations reported here can tune the efficacy of Ca^{2+}-triggered exocytosis and/or alter the frequency of spontaneous SV fusion events (17).

Acknowledgment—We thank the members of the Chapman laboratory for critical review of this manuscript and several helpful discussions.

REFERENCES

1. Katz, B., and Miledi, R. (1965) *Proc. R. Soc. Lond. B. Biol. Sci.* **161,** 496–503
2. Rothman, J. E. (1994) *Nature* **372,** 55–63
3. Chapman, E. R. (2008) *Ann. Rev. Biochem.* **77,** 615–641
4. Perin, M. S., Brose, N., Jahn, R., and Sudhof, T. C. (1991) *J. Biol. Chem.* **266,** 623–629
5. Chapman, E. R., and Davis, A. F. (1998) *J. Biol. Chem.* **273,** 13995–14001
6. Bai, J., Wang, P., and Chapman, E. R. (2002) *Proc. Natl. Acad. Sci. U. S. A.* **99,** 1665–1670
7. Bai, J., Tucker, W. C., and Chapman, E. R. (2004) *Nat. Struct. Mol. Biol.* **11,** 36–44
8. Bhalla, A., Tucker, W. C., and Chapman, E. R. (2005) *Mol. Biol. Cell* **16,** 4755–4764
9. Schiavo, G., Stenbeck, G., Rothman, J. E., and Sollner, T. H. (1997) *Proc. Natl. Acad. Sci. U. S. A.* **94,** 997–1001
10. Chapman, E. R., Hanson, P. I., An, S., and Jahn, R. (1995) *J. Biol. Chem.* **270,** 23667–23671
11. Bai, J., Wang, C. T., Richards, D. A., Jackson, M. B., and Chapman, E. R. (2004) *Neuron* **41,** 929–942
12. Lynch, K. L., Gerona, R. R., Larsen, E. C., Marcia, R. F., Mitchell, J. C., and Martin, T. F. (2007) *Mol. Biol. Cell* **18,** 4957–4968
13. Shin, O. H., Rhee, J. S., Tang, J., Sugita, S., Rosenmund, C., and Sudhof, T. C. (2003) *Neuron* **37,** 99–108
14. Shin, O. H., Maximov, A., Lim, B. K., Rizo, J., and Sudhof, T. C. (2004) *Proc. Natl. Acad. Sci. U. S. A.* **101,** 2554–2559
15. Shin, O. H., Rizo, J., and Sudhof, T. C. (2002) *Nat. Neurosci.* **5,** 649–656
16. Popov, S. V., and Poo, M. M. (1993) *Cell* **73,** 1247–1249
17. Chicka, M. C., Hui, E., Liu, H., and Chapman, E. R. (2008) *Nat. Struct. Mol. Biol.* **15,** 827–835
18. Weber, T., Zemelman, B. V., McNew, J. A., Westermann, B., Gmachl, M., Parlati, F., Sollner, T. H., and Rothman, J. E. (1998) *Cell* **92,** 759–772
19. Tucker, W. C., Weber, T., and Chapman, E. R. (2004) *Science* **304,** 435–438
20. Bhalla, A., Chicka, M. C., Tucker, W. C., and Chapman, E. R. (2006) *Nat. Struct. Mol. Biol.* **13,** 323–330
21. Mackler, J. M., Drummond, J. A., Loewen, C. A., Robinson, I. M., and Reist, N. E. (2002) *Nature* **418,** 340–344
22. Robinson, I. M., Ranjan, R., and Schwarz, T. L. (2002) *Nature* **418,** 336–340
23. Stevens, C. F., and Sullivan, J. M. (2003) *Neuron* **39,** 299–308
24. Nishiki, T., and Augustine, G. J. (2004) *J. Neurosci.* **24,** 8542–8550
25. Littleton, J. T., Stern, M., Perin, M., and Bellen, H. J. (1994) *Proc. Natl. Acad. Sci. U. S. A.* **91,** 10888–10892
26. Loewen, C. A., Lee, S. M., Shin, Y. K., and Reist, N. E. (2006) *Mol. Biol. Cell* **17,** 5211–5226
27. Li, L., Shin, O. H., Rhee, J. S., Arac, D., Rah, J. C., Rizo, J., Sudhof, T., and Rosenmund, C. (2006) *J. Biol. Chem.* **281,** 15845–15852
28. Stein, A., Radhakrishnan, A., Riedel, D., Fasshauer, D., and Jahn, R. (2007) *Nat. Struct. Mol. Biol.* **14,** 904–911
29. Martens, S., Kozlov, M. M., and McMahon, H. T. (2007) *Science* **316,** 1205–1208
30. Chapman, E. R., An, S., Edwardson, J. M., and Jahn, R. (1996) *J. Biol. Chem.* **271,** 5844–5849
31. Bowen, M. E., Weninger, K., Ernst, J., Chu, S., and Brunger, A. T. (2005) *Biophys. J.* **89,** 690–702
32. Shao, X., Li, C., Fernandez, I., Zhang, X., Sudhof, T. C., and Rizo, J. (1997) *Neuron* **18,** 133–142
33. Fernandez, I., Ubach, J., Dulubova, I., Zhang, X., Sudhof, T. C., and Rizo, J. (1998) *Cell* **94,** 841–849
34. Wang, P., Wang, C. T., Bai, J., Jackson, M. B., and Chapman, E. R. (2003) *J. Biol. Chem.* **278,** 47030–47037
35. Sutton, R. B., Davletov, B. A., Berghuis, A. M., Sudhof, T. C., and Sprang, S. R. (1995) *Cell* **80,** 929–938
36. Sutton, R. B., Fasshauer, D., Jahn, R., and Brunger, A. T. (1998) *Nature* **395,** 347–353
37. Fuson, K. L., Montes, M., Robert, J. J., and Sutton, R. B. (2007) *Biochemistry* **46,** 13041–13048

38. Desai, R. C., Vyas, B., Earles, C. A., Littleton, J. T., Kowalchyck, J. A., Martin, T. F., and Chapman, E. R. (2000) *J. Cell Biol.* **150,** 1125–1136
39. Breckenridge, W. C., Gombos, G., and Morgan, I. G. (1972) *Biochim. Biophys. Acta* **266,** 695–707
40. Breckenridge, W. C., Morgan, I. G., Zanetta, J. P., and Vincendon, G. (1973) *Biochim. Biophys. Acta* **320,** 681–686
41. Tucker, W. C., Edwardson, J. M., Bai, J., Kim, H. J., Martin, T. F., and Chapman, E. R. (2003) *J. Cell Biol.* **162,** 199–209
42. Szoka, F., Jr., and Papahadjopoulos, D. (1980) *Annu. Rev. Biophys. Bioeng.* **9,** 467–508
43. Rickman, C., and Davletov, B. (2003) *J. Biol. Chem.* **278,** 5501–5504
44. Fontaine, R. N., Harris, R. A., and Schroeder, F. (1980) *J. Neurochem.* **34,** 269–277
45. Chernomordik, L., and Kozlov, M. (2003) *Ann. Rev. Biochem.* **72,** 175–207
46. Dai, H., Shen, N., Arac, D., and Rizo, J. (2007) *J. Mol. Biol.* **367,** 848–863
47. Nalefski, E. A., and Falke, J. J. (1996) *Protein Sci.* **5,** 2375–2390
48. Jackson, M. B., and Chapman, E. R. (2006) *Ann. Rev. Biophys. Biomol. Struct.* **35,** 135–160